

EPR of Transient Free Radicals during Photochemical Reactions in High Temperature and Pressure Gases

S. N. Batchelor, B. Henningsen, and H. Fischer*

Physikalisch-Chemisches Institut der Universität Zürich, Winterthurerstrasse 190, CH-8057 Zürich, Switzerland

Received: October 17, 1996; In Final Form: February 11, 1997[⊗]

Well-resolved EPR spectra are reported for transient organic radicals produced by photolysis of ketones in gas phase solutions at pressures and temperatures of up to 150 bar and 720 K. Under these conditions α -cleavage is more important than at ambient temperatures, and for excited acetone the rate constant is estimated as $\geq 7 \times 10^7 \text{ s}^{-1}$ at 600 K and 140 bar. The EPR line widths are found to be controlled by spin-rotational interaction and are well predicted from theory for radicals with radii $>0.25 \text{ nm}$. Analysis of the hydroxy-proton coupling of the 2-hydroxy-2-propyl radical gives a rotation barrier of 18.1 kJ mol^{-1} about the $\text{C}_\alpha\text{-OH}$ bond. This increases to 22.7 kJ mol^{-1} on addition of acetone which is attributed to hydrogen bonding.

Introduction

Radicals are important intermediates in many chemical and biological processes, and electron paramagnetic resonance (EPR) spectroscopy allows their direct identification.¹ So far, EPR has been confined mainly to radicals in condensed phases, though they are also extremely important in gas phase reactions, such as pyrolysis and combustion.² This situation may have arisen because of a general belief that the spin-rotational interaction leads to extreme broadening of EPR resonances for nearly all polyatomic radical species in the gas phase. However, Schaafsma and Kivelson found resolved hyperfine structure for a stable gas phase nitroxide radical provided a high pressure was applied.³ This increases the collisional relaxation of the rotational angular momentum and hence narrows the EPR lines. Livingston and Zeldes have extended this work to large sized transient organic radicals formed by pyrolysis above the critical point of the solvents^{4,5} and obtained line widths of $10\text{--}50 \mu\text{T}$. Recently, Krusic *et al.* also reported gas phase EPR spectra of some persistent radicals.⁶

Here, we present results of a gas phase EPR study aiming at medium and small sized transient radicals produced by photolysis or pyrolysis above the critical point of the solvents. The use of photolysis under such conditions is also novel, though a few related results have been reported for the high temperature liquid phase.⁵

Experimental Section

The apparatus is based on the design of Livingston and Zeldes.⁷ A solution is deoxygenated by helium purging and then pumped through a high pressure flow system with a HPLC pump (SMI Concept Series III) at rates of typically $0.5\text{--}1 \text{ mL min}^{-1}$. Stainless steel high pressure connecting tubing is used except for a quartz capillary section (Heralux, o.d. = 4.8 mm , i.d. = 1.4 mm) which traverses the TE102 cavity of the EPR spectrometer (Bruker X-band ESP 300). The metal to glass connections follow a published design.⁷ The pressure is controlled by a needle valve and is measured by the pump's transducer and a second one just before the needle valve. In room temperature tests the capillary shattered at pressures of $300\text{--}350 \text{ bar}$, the actual capillary used for high temperature experiments was tested at 200 bar for 1 h , and 150 bar was set as the maximum pressure using the safety trip of the HPLC pump.

The sample is heated using a commercial device (Wilmad WG-838, 836) by flowing hot nitrogen at 15 L min^{-1} through the EPR Dewar surrounding the capillary. The temperature is measured with a thermocouple between the Dewar and the capillary at the top of the cavity and gives the temperature of the nitrogen. A temperature-dependent correction factor is applied to take account of the drop in temperature between the center and the top of the cavity. Given temperatures are estimated to be accurate to $\pm 10 \text{ K}$. Thus far, temperatures up to 800 K were achieved, though this is not the maximum obtainable. Occasionally, a black paramagnetic deposit collected on the inner capillary wall. This was removed by flowing 4 M HNO_3 at 450 K and 70 bar for 30 min .

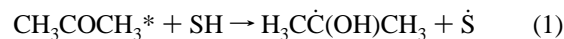
Irradiation of the sample uses the filtered light (aqueous Ni/Co sulfate, $260 \text{ nm} < \lambda < 340 \text{ nm}$) of a 1000 W Hg-Xe lamp (Hanovia) focused onto the sample through the irradiation port of the EPR cavity. The front and back plates of the cavity were altered to include water cooling. Extra signals at $g \sim 2$ arise from the quartz and from radicals absorbed on it.

The ketones were obtained in their purest available commercial forms and the solvents in HPLC grade and used as supplied. The solutions used contained $5\text{--}10 \text{ vol } \%$ ketone.

Results and Discussion

Observed Radicals and Reactions. Figure 1 shows EPR spectra obtained during photolysis of acetone in propan-2-ol and toluene. They were recorded above the critical points of the solvents, which are 508 K , 53.1 bar and 594 K , 41.1 bar for propan-2-ol and toluene, respectively,⁸ and are due to radicals derived by hydrogen abstraction from the solvents, i.e., 2-hydroxy-2-propyl and benzyl. Analogously, with cyclopentane, methanol, and ethanol at 600 K and 140 bar , cyclopentyl, hydroxymethyl, and 1-hydroxy-1-ethyl radicals were detected. Interestingly, at room temperature the photolysis of acetone in toluene, cyclopentane, methanol, and ethanol leads to the observation of both the solvent-derived and the acetone-derived 2-hydroxy-2-propyl radicals, whereas at high temperature only the solvent-derived species are detected.

It is well-known that at room temperature excited acetone predominantly reacts by a photoreduction reaction with all of the solvents, SH, used here.⁹



[⊗] Abstract published in *Advance ACS Abstracts*, April 1, 1997.

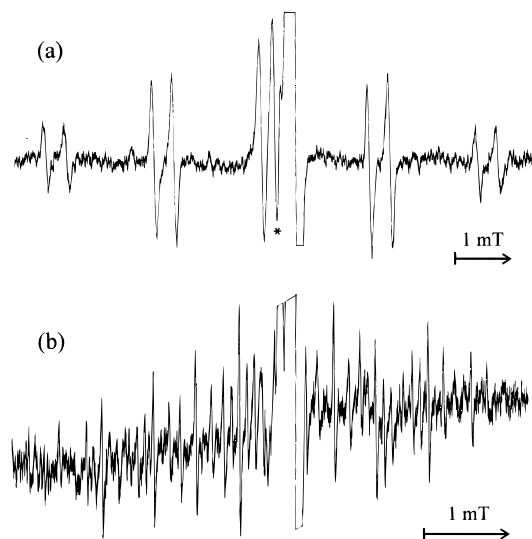
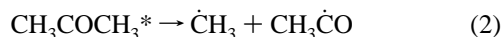


Figure 1. EPR spectra obtained by photolysis of 10% acetone solutions in (a) propan-2-ol at 580 K and 140 bar and (b) toluene at 630 K and 140 bar. Only the central five pairs of lines of the 2-hydroxy-2-propyl radical are shown in (a). The large central signal is thought to be due to radicals absorbed on the capillary walls. The signal marked with an asterisk arises from the Dewar.

Except for propan-2-ol, this process cannot explain the high temperature and pressure spectra, since 2-hydroxy-2-propyl radicals are not observed, and therefore, a change in mechanism with temperature must occur.

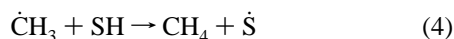
Presumably at the high temperatures excited acetone undergoes α -cleavage more rapidly than at room temperature



and the acetyl radical decarbonylates, thereafter. At 600 K this process has a rate constant of $8.5 \times 10^6 \text{ s}^{-1}$.¹⁰



The methyl radical then abstracts a hydrogen atom from the solvent to give the observed species.



Arrhenius parameters for this reaction¹¹ give a rate constant, k_{abs} , of $2 \times 10^5 \text{ M}^{-1} \text{ s}^{-1}$ for both conditions given in Figure 1. The molarity of the solvents is estimated using the ideal gas law as 3 M, and hence reaction 4 is rapid enough to explain the results. Due to the small size of the methyl radical, its EPR line is estimated (*vide infra* Figure 3b) to be broadened to ~ 0.2 mT by the spin-rotational interaction. When this is combined with the short lifetime due to reaction 4, methyl becomes unobservable under our conditions.

The Arrhenius parameters for reaction 1 are not known; however, they have been measured for acetophenone,¹² which has similar rate constants as acetone at room temperature.¹³ Using the values for cyclohexane as solvent gives a rate constant of $7 \times 10^6 \text{ M}^{-1} \text{ s}^{-1}$ at 600 K, which when combined with the concentration of solvent, 3 M, leads to a photoreduction lifetime of 50 ns for excited acetone. For 2-hydroxy-2-propyl radicals to be unobservable the α -cleavage must occur at least 3–4 times faster than this; i.e., the rate constant must be larger than $7 \times 10^7 \text{ s}^{-1}$ at 600 K. This value is greater than predicted from low pressure (0.26 bar) gas phase data of $3 \times 10^6 \text{ s}^{-1}$; however, α -cleavage is known to become faster with increasing pressure.¹⁴

This change in mechanism from photoreduction to α -cleavage is also strongly supported by the GLC observation of methane

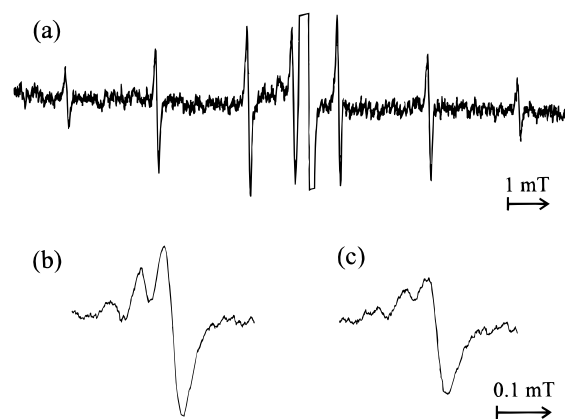


Figure 2. (a) EPR spectra obtained by photolysis of di-*tert*-butyl ketone in benzene at 610 K and 140 bar. Only the central six lines of the *tert*-butyl radical are shown. One line is shown with greater resolution in (b) and again, but at 50 bar, in (c).

as the major reaction product at 600 K, 140 bar but not at ambient temperature and pressure. It exemplifies an expected trend in radical and excited state chemistry. At high temperatures, the rate constants will approach the frequency factor limit, which for fragmentation reactions is typically $A \sim 10^{11} - 10^{14} \text{ s}^{-1}$, and for hydrogen transfer (and radical addition reactions) $A \sim 10^6 - 10^9 \text{ M}^{-1} \text{ s}^{-1}$.^{15,16} Consequently, at high temperatures the fragmentations will dominate for usual solvent concentrations.

Photoreactions of several other ketones were also investigated. Photolysis of di-*tert*-butyl ketone in benzene produced *tert*-butyl radicals in an analogous manner to the reactions 2 and 3 of acetone, Figure 2a, and second-order hyperfine structure could be detected, Figure 2b,c. Photolysis in propan-2-ol led to the observation of 2-hydroxy-2-propyl and *tert*-butyl radicals in a concentration ratio of 7:2 at 580 K and 140 bar. The radical termination constant, $2k_t$, may be extrapolated from the mean for the two radicals of $1.5 \times 10^9 \text{ M}^{-1} \text{ s}^{-1}$ at 298 K^{17,18} to $1.5 \times 10^{11} \text{ M}^{-1} \text{ s}^{-1}$ at 580 K, as k_t is proportional to T/η for liquids and high pressure gases.^{18,19} Calibration of the spectrometer indicates a radical concentration of $2 \times 10^{-7} \text{ M}$, which is approximately 1 order of magnitude lower than that attainable at room temperature.²⁰ In a simple steady state photochemical scheme where radicals are created at a constant rate and only self-terminate, the radical concentration should be proportional to $(2k_t)^{-1/2}$. This predicts a drop in radical concentration by a factor of 10 between 298 and 580 K, as observed. From these data an abstraction rate constant of $3 \times 10^4 \text{ M}^{-1} \text{ s}^{-1}$ is estimated, which is much higher than that predicted from Arrhenius parameters of $7 \times 10^2 \text{ M}^{-1} \text{ s}^{-1}$.²⁰ The Arrhenius parameters were extracted from data obtained between 299 and 354 K, and the large extrapolation required may explain the discrepancy.

Photolysis of 2,4-dimethylpentan-3-one follows an analogous pattern to acetone and di-*tert*-butyl ketone. Here, hydrogen abstraction from the ketone itself by the 2-propyl radical proved to be an important reaction. In benzene the predominant signal arose from the 2,4-dimethyl-2-pentan-3-oyl radical with a smaller signal from the 2-propyl radical. At 620 K and 8% ketone the radicals appeared in the ratio 2:1, which when combined with the estimate for the total radical concentration and $2k_t$ gives an abstraction rate constant of approximately $1 \times 10^5 \text{ M}^{-1} \text{ s}^{-1}$.

Photoreduction of the excited ketone was found dominant for acetophenone in propan-2-ol, and at temperatures up to 720 K the 1-hydroxy-1-phenyl-1-ethyl radical was observed. As at room temperature, the 2-hydroxy-2-propyl radicals were absent, due to their rapid hydrogen atom transfer to acetophenone.⁹

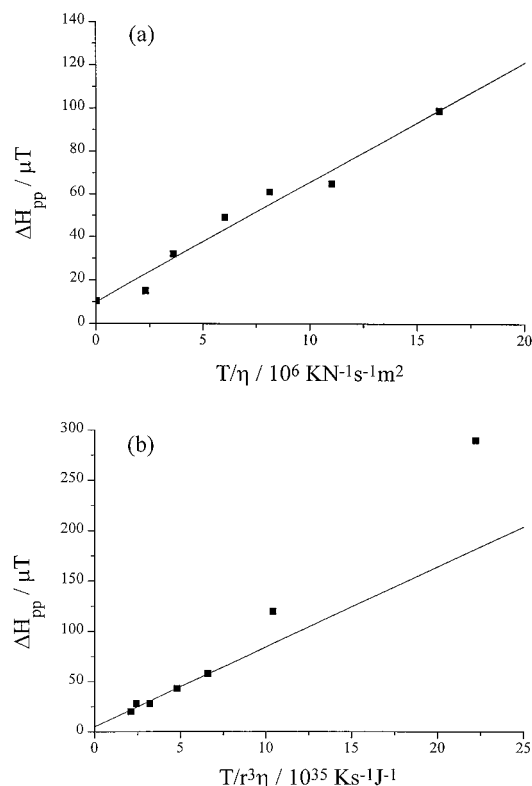


Figure 3. (a) Variation of the 2-hydroxy-2-propyl radical linewidth with T/η . (b) Variation of line widths with $T/r^3\eta$. From left to right the radicals are diphenylmethyl, 1-hydroxy-1-phenyl-1-ethyl, benzyl, *tert*-butyl, 2-hydroxy-2-propyl, 1-hydroxy-1-ethyl, and hydroxymethyl.

TABLE 1: Variation of Line Width with Radical at 140 bar^a

radical	r/nm	T/K	$\eta/10^{-6}$ N s m^{-2}	$\Delta H_{\text{pp}}/\mu\text{T}$	$\tau_1/10^{-13}$ s	$\tau_2/10^{-13}$ s
CH_2OH	0.19	550	36	290	3.0	1.4
$\text{CH}_3\dot{\text{C}}\text{HOH}$	0.23	570	45	120	2.9	2.9
$(\text{CH}_3)_2\dot{\text{C}}\text{OH}$	0.26	580	50	60	3.0	4.6
$(\text{CH}_3)_3\dot{\text{C}}$	0.28	610	58	43	2.3	6.3
$\text{Ph}\dot{\text{C}}\text{H}_2$	0.315	630	79	28	2.4	11.9
$\text{Ph}\dot{\text{C}}(\text{OH})\text{CH}_3$	0.33	580	50	28	4.9	14.1
$\text{Ph}_2\dot{\text{C}}$	0.38	700	60	20	4.9	16.1

^a Radii were taken from the literature^{17,18} or estimated using refs 27 and 28. Viscosities were taken directly from, or by extrapolation of, literature data.⁸ Values of η and ΔH_{pp} are estimated to be accurate to $\pm 10\%$.

As in previous work,⁴ the pyrolysis of neat diphenylmethane in benzene at 700 K was investigated, and diphenylmethyl radicals were observed due to an unknown mechanism. Also, 2-hydroxy-2-propyl radicals were found during thermolysis of 5% di-*tert*-butyl peroxide in propan-2-ol in the temperature range 440–530 K.

Line Widths. Figures 1–3 and Table 1 show that the EPR line widths vary markedly with radical, temperature, and pressure. Electron spin relaxation in the gas phase is thought to be mainly due to the spin–rotation interaction. For an axially symmetric radical at X-band ($\omega\tau \ll 1$) in a fluid this contribution is²¹

$$(T_1)^{-1} = (T_2)^{-1} = 2IkT/9\hbar^2 \{ (2C_{\perp} + C_{\parallel})^2 \tau_1 + 2(C_{\parallel} - C_{\perp})^2 \tau_{12} \} \quad (5)$$

where C_{\parallel} and C_{\perp} are the diagonal components of the spin–rotational interaction tensor, I is the moment of inertia of the radical, T is the temperature, and τ_1 is the rotational correlation

time. In high pressure gases diffusional behavior occurs since the mean free path is not large compared to the interparticle distance. Thus, τ_1 may be estimated from

$$\tau_1 = I/8\pi r^3 \eta \quad (6)$$

where η is the viscosity of the fluid. τ_{12} is given by

$$(\tau_{12})^{-1} = (\tau_1)^{-1} + (\tau_2)^{-1} \quad (7)$$

where τ_2 is the reorientational correlation time

$$\tau_2 = 4\pi r^3 \eta / 3kT \quad (8)$$

The second term in eq 5 is only valid if the reorientational and rotational motions are not correlated, i.e., when $\tau_1 \gg \tau_2$ or $\tau_2 \gg \tau_1$. In the latter limit, eq 5 may be simplified to²²

$$(T_2)^{-1} = (12\pi r^3)^{-1} (\Delta g_{\parallel}^2 + 2\Delta g_{\perp}^2) kT / \eta \quad (9)$$

where $\Delta g = g - 2.00231$ for the parallel and perpendicular components of the radical's g tensor.

Equation 9 describes the line widths quantitatively in many of the cases discussed here. For 2-hydroxy-2-propyl a linear increase of the peak-to-peak line width, ΔH_{pp} , with T/η was found (Figure 3a). Using the literature value of 0.26 nm for the radius of the radical¹⁷ and assuming a Gaussian line shape, the slope leads to $\Delta g_{\parallel}^2 + 2\Delta g_{\perp}^2 = 3.8 \times 10^{-6}$. Unfortunately, the g factor anisotropy of 2-hydroxy-2-propyl is unknown, but from analogous radicals²³ a value of $(2-4) \times 10^{-6}$ is expected. For radicals with line widths not affected by unresolved couplings and with $r > 0.25$ nm (Table 1), a linear correlation with $T/r^3\eta$ was found (Figure 3b). Here the slope leads to $\Delta g_{\parallel}^2 + 2\Delta g_{\perp}^2 = 3.0 \times 10^{-6}$, again as expected. The excellent accord between theory and experiment is surprising since eq 9 is valid only for $t_2 \gg \tau_1$, which from the data of Table 1 does not appear to be the case. This suggests that eq 8 may underestimate the reorientational correlation time under these conditions. For the relatively small hydroxymethyl and 1-hydroxy-1-ethyl radicals a reorientational contribution to relaxation is important and leads to a significant increase in line width beyond that predicted by eq 9.

A detailed investigation of the pressure dependence of the line width was not conducted because the changes were rather small in the measurable range. Nevertheless, an effect is seen in the second-order structure of the *tert*-butyl radical (Figure 2b,c). On decreasing the pressure from 140 to 50 bar the line width of *tert*-butyl increases from 43 to 53 μT , which matches the increase in η^{-1} from 1.7×10^4 to $2.1 \times 10^4 \text{ N}^{-1} \text{ s}^{-1} \text{ m}^2$.⁸

Hyperfine Coupling Constants. Most coupling constants of the observed radicals agree well with room temperature data.²⁴ An exception is the hydroxy–proton coupling of the 2-hydroxy-2-propyl radical which increases almost linearly with temperature in the range 280–710 K from 0.05 to 0.48 mT. This behavior was previously reported for a much narrower temperature range and assigned to an increase of the rotation rate about the $\text{C}_a\text{--OH}$ bond.^{25,26} A marked difference of the temperature dependence is observed when the radical was produced thermally by di-*tert*-butyl peroxide and by photoreaction of acetone (Figure 4). In the thermal experiments addition of acetone caused a decrease of the hyperfine coupling. This points to an interaction, probably a hydrogen bond between the 2-hydroxy-2-propyl radical and the ketone, that increases the barrier to rotation even at high temperatures.

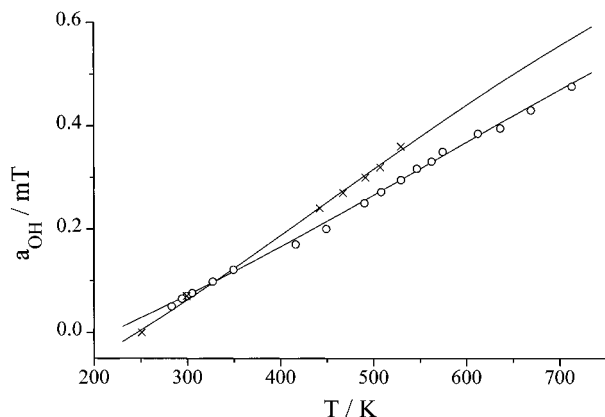


Figure 4. (a) Variation of hydroxy-proton coupling of the 2-hydroxy-2-propyl radical with temperature. The radical was produced by acetone photolysis (O) and di-*tert*-butyl peroxide pyrolysis (x); values below 360 K taken from refs 17 and 25.

The temperature dependence of the coupling constant, $a_{\text{OH}}(T)$, was analyzed by a classical approach via²⁶

$$a_{\text{OH}}(T) = \frac{\int_{-\pi}^{\pi} a_{\text{OH}}(\theta) \exp[-V(\theta)/kT] d\theta}{\int_{-\pi}^{\pi} \exp[-V(\theta)/kT] d\theta} \quad (10)$$

Here, $a_{\text{OH}}(\theta)$ is the variation of coupling constant with angle of rotation, θ ,

$$a_{\text{OH}}(\theta) = A + B \cos^2(\theta + \pi/2) \quad (11)$$

and $V(\theta)$ is the potential function representing the barrier to rotation, of height V_2 .

$$V(\theta) = V_2(1 - \cos 2\theta)/2 \quad (12)$$

The value of $B = 4.15$ mT was taken from the literature,²⁶ and fits of the experimental data to eq 10 then gave $A = -0.17$ and -0.25 mT and $V_2 = 22.7$ and 18.1 kJ mol⁻¹ for the photolytic and thermal data, respectively. A similar barrier of $V_2 = 16.7$ kJ mol⁻¹ is known for the hydroxymethyl radical.²⁶

The 1-hydroxy-1-phenyl-1-ethyl radical's methyl and hydroxy couplings also showed a strong temperature dependence, increasing from 1.41 and 0.06 mT at 276 K⁹ to 1.46 and 0.48 mT at 610 K, respectively.

Concluding Remark

Extending the pioneering work of Livingston and Zeldes^{4,5,7} on benzylic radicals, i.e., fairly large transient species, we have

shown that transient radicals even as small as hydroxymethyl can be detected by EPR in high pressure and temperature gases. Due to the unfavorable temperature and filling factor, the signal intensities are at the detection limit of present spectrometers but may possibly be improved by additional optimization. Hence, EPR may become widely applicable in the study of the mechanisms and kinetics of radical reactions in the gas phase as it is for the condensed phases.

Acknowledgment. The authors thank Mr. A. Kühne and Mr. D. Schnarwiler for technical and glass blowing assistance, respectively, in the construction of the apparatus and Prof. H. Paul for useful discussions (all Zurich University). Mrs. I. Verhoolen is thanked for the GLC analysis (Zurich University). Financial support by the Swiss National Foundation for Scientific Research is gratefully acknowledged.

References and Notes

- (1) Atherton, N. M. *Principles of Electron Spin Resonance*; Ellis Horwood: London, 1993.
- (2) Benson, S. W. *Thermochemical Kinetics*, 2nd ed. John Wiley and Sons: New York, 1976.
- (3) Schaafsma, T. J.; Kivelson, D. *J. Chem. Phys.* **1968**, *49*, 5235.
- (4) Livingston, R.; Zeldes, H.; Conradi, M. S. *J. Am. Chem. Soc.* **1979**, *101*, 4312.
- (5) Livingston, R.; Zeldes, H. *J. Phys. Chem.* **1983**, *87*, 1086.
- (6) Krusic, P. J.; Kating, P. M.; Roe, D. C. Presented at the VII International Symposium on Organic Free Radicals, Bardolino, Italy, 1996.
- (7) Livingston, R.; Zeldes, H. *Rev. Sci. Instrum.* **1981**, *52*, 1352.
- (8) Stephan, K.; Lucas, K. *Viscosity of Dense Fluids*; Plenum Press: New York, 1979.
- (9) Paul, H.; Fischer, H. *Helv. Chim. Acta* **1973**, *56*, 2011.
- (10) Vollenweider, J. K.; Paul, H. *Int. J. Chem. Kinet.* **1986**, *18*, 791.
- (11) Benson, S. W. *Adv. Photochem.* **1964**, *2*, 2.
- (12) Giering, L.; Berger, M.; Steel, C. *J. Am. Chem. Soc.* **1974**, *96*, 953.
- (13) Berger, M.; McAlpine, E.; Steel, C. *J. Am. Chem. Soc.* **1978**, *100*, 5147.
- (14) Porter, G.; Dogra, S. K.; Loutfy, R. O.; Sugamori, S. E.; Yip, R. W. *J. Chem. Soc., Faraday Trans. 1* **1973**, *69*, 1462.
- (15) O'Neal, H. E.; Larson, C. W. *J. Phys. Chem.* **1969**, *73*, 1011.
- (16) *Handbook of Organic Photochemistry*; Scaiano, J. C., Ed.; CRC Press: Boca Raton, FL, 1989; Vol. II.
- (17) Landolt-Börnstein. *Radical Reaction Rates in Liquids*; Fischer, H., Ed.; New Series; Springer-Verlag: Berlin, 1995; Vol. II/18a&b.
- (18) Lezni, M.; Fischer, H. *Int. J. Chem. Kinet.* **1983**, *15*, 733.
- (19) Schuh, H.; Fischer, H. *Helv. Chim. Acta* **1978**, *61*, 2463.
- (20) Troe, J. *J. Phys. Chem.* **1986**, *90*, 357.
- (21) Münger, K.; Fischer, H. *Int. J. Chem. Kinet.* **1985**, *17*, 809.
- (22) Hubbard, P. S. *Phys. Rev.* **1963**, *131*, 1155.
- (23) Atkins, P. W.; Kivelson, D. *J. Chem. Phys.* **1965**, *44*, 169.
- (24) Griffith, O. H. *J. Chem. Phys.* **1965**, *42*, 2651. Birrell, G. B.; Griffith, O. H. *J. Phys. Chem.* **1971**, *75*, 3489.
- (25) Landolt-Börnstein. *Magnetic Properties of Free Radicals*; Fischer H., Hellwege, K.-H., Eds.; Springer-Verlag: Berlin, 1977.
- (26) Livingston, R.; Zeldes, H. *J. Chem. Phys.* **1966**, *44*, 1245.
- (27) Krusic, P. J.; Meakin, P.; Jesson, J. P. *J. Phys. Chem.* **1971**, *75*, 3438.
- (28) Spornol, A.; Wirtz, K. *Naturforsch., A* **1953**, *8*, 522.
- (29) Edwards, J. T. *J. Chem. Educ.* **1970**, *47*, 261.